

AA-SVD: ANCHORED AND ADAPTIVE SVD FOR LARGE MODEL COMPRESSION

005 **Anonymous authors**

006 Paper under double-blind review

ABSTRACT

011 Pretrained large-language and vision-language models have demonstrated remarkable
 012 capabilities over the years, but their ever-increasing size poses challenges for
 013 deployment and accessibility. Model compression offers a path toward democratizing
 014 access, yet many existing approaches either require costly retraining or
 015 result in substantial performance degradation. To address this, we introduce a fast
 016 SVD-based truncation framework for compressing pretrained networks that en-
 017 ables rapid compression of billion-parameter models without retraining. Unlike
 018 existing SVD-based approaches that optimize only on the original inputs — ig-
 019 noring distribution shifts from upstream compression and thus propagating errors
 020 forward—or those that rely only on shifted inputs and risk drifting away from
 021 the original outputs, our approach accounts for both. By anchoring each com-
 022 pressed layer to the original outputs while explicitly modeling input distribution
 023 shifts, our method identifies optimal low-rank approximations that maintain func-
 024 tional equivalence with the uncompressed network, thereby preserving the behav-
 025 ior of the full model. Experiments across language and vision-language mod-
 026 els of varying scales demonstrate that our method not only achieves favorable
 027 trade-offs between compression ratio and task accuracy, but also outperforms ex-
 028 isting baselines particularly at low compression ratios—where the gap widens as
 029 compression becomes more aggressive—offering a practical solution for efficient,
 030 large-scale model deployment.

1 INTRODUCTION

033 The rapid progress of large-scale pretrained models has fundamentally transformed natural language
 034 processing and multimodal learning. Modern large language models (LLMs) (Touvron et al., 2023;
 035 Zhang et al., 2022; Achiam et al., 2023) and vision-language models (VLMs) (Radford et al., 2021;
 036 Liu et al., 2023; Dosovitskiy et al., 2021) now routinely contain billions of parameters, enabling
 037 strong generalization capabilities across a wide range of downstream tasks. However, this improve-
 038 ment in performance has come at the cost of scale: training, fine-tuning, and inference with such
 039 models often requires clusters of high-memory GPUs, making them prohibitively expensive to de-
 040 ploy in resource-constrained or latency-sensitive settings. As model sizes continue to grow, practical
 041 challenges around cost, efficiency, and accessibility become even more pressing Kaplan et al. (2020);
 042 Patterson et al. (2021).

043 One promising direction is to move beyond ever-larger models toward smaller, more efficient ones.
 044 Compact models can be trained from scratch for specialized tasks, but this approach sacrifices the
 045 broad generalization ability of large pretrained networks. Alternatively, smaller models can be ob-
 046 tained by *distilling* large networks into student models trained to mimic their behavior (Hinton et al.,
 047 2015; Xu et al., 2024), or by applying *post-training compression* techniques such as pruning, quan-
 048 tization, or low-rank factorization (Cheng et al., 2017; Zhu et al., 2024). While both approaches
 049 reduce memory footprint and inference cost, distillation typically requires substantial retraining data
 050 and compute (Jiao et al., 2020; Touvron et al., 2021), whereas post-training compression can often be
 051 applied more rapidly to pretrained networks (Frantar et al., 2022; Dettmers et al., 2022; Wang et al.,
 052 2025c), thereby offering a practical path towards democratizing deployment. These compressed
 053 models can either be deployed directly for efficient inference, fine-tuned to adapt to downstream
 tasks, or embedded within distributed systems that demand low-latency and high-throughput infer-
 ence.

054 A wide range of model compression techniques have been proposed, spanning distinct methodolog-
 055 ical families. *Pruning* removes redundant weights or structures from neural networks, with early
 056 work on unstructured sparsification (Han et al., 2015) and the lottery ticket hypothesis (Frankle
 057 & Carbin, 2019) showing that smaller subnetworks can be retrained to match dense counterparts.
 058 While effective, pruning often requires iterative retraining and specialized sparsity-aware hardware
 059 to fully realize efficiency gains, though recent advances such as SparseGPT and its variants (Frantar
 060 & Alistarh, 2023; Ma et al., 2023; Ashkboos et al., 2024; An et al., 2024) have enabled post-training
 061 pruning of large language models. *Quantization* reduces numerical precision of weights and activa-
 062 tions, thereby shrinking memory footprint and accelerating inference. Classic approaches demon-
 063 strated the feasibility of quantized neural networks (Hubara et al., 2017), while modern methods
 064 like LLM.int8() (Dettmers et al., 2022), QLoRA (Dettmers et al., 2023), and AWQ (Lin et al., 2024)
 065 allow near-lossless compression of transformers. However, quantization methods may require care-
 066 ful calibration and sometimes introduce instability for very low-bit settings. Another line of work
 067 leverages the inherent low-rank structure of network weights: *low-rank factorization* decomposes
 068 large matrices into compact representations, reducing both parameters and computation. Early ap-
 069 plications in CNNs (Denton et al., 2014; Tai et al., 2015) demonstrated significant speedups, but
 070 naïve SVD truncation is known to degrade accuracy. More recent activation-aware approaches for
 071 LLMs (Yuan et al., 2023; Wang et al., 2025d; Li et al., 2025; Wang et al., 2025a; Li et al., 2025) ex-
 072 plicitly account for input activations, mitigating this limitation at the cost of additional computation.
 073

074 These methods differ in their retraining requirements, their dependence on large datasets versus
 075 small calibration samples, the efficiency with which compression can be applied to pretrained net-
 076 works, the degree to which downstream accuracy is preserved, and the extent to which the resulting
 077 compressed structure aligns with modern accelerators (Cheng et al., 2018). Among these, *SVD-
 078 based methods* are especially appealing: they exploit the inherent low-rank structure of neural net-
 079 work weights, yielding compressed models without the need for expensive retraining (Denton et al.,
 080 2014; Jaderberg et al., 2014). A straightforward approach is to directly truncate weight matrices
 081 by retaining only the top singular components, but this often leads to severe degradation because it
 082 treats all input directions equally and discards information that is important for the actual distribu-
 083 tion of activations (Denil et al., 2013; Chen et al., 2021; Wang et al., 2025d). This limitation has
 084 been repeatedly observed in large-scale networks, where naïve low-rank truncation fails to preserve
 085 task accuracy and generalization. To address this, activation-aware approaches have been developed
 086 that tailor the factorization to the input distribution, thereby retaining the directions most relevant to
 087 the network’s operation. However, existing activation-aware SVD methods often optimize low-rank
 088 approximations using only the original input distribution (Yuan et al., 2023; Wang et al., 2025d; Li
 089 et al., 2025; Wang et al., 2025a), ignoring the shift introduced by upstream compression, which can
 090 propagate errors and degrade downstream performance. Conversely, methods that rely exclusively
 091 on shifted inputs, such as DobiSVD (Wang et al., 2025a), risk deviating from the original network
 092 behavior, introducing instability and loss of fidelity.

093 In this work, we present **AA-SVD**, a *fast SVD-based truncation framework* for compressing pre-
 094 trained networks. Unlike existing SVD truncation or activation-aware methods that only consider
 095 a single input distribution, our approach accounts for both the original outputs and the distribution
 096 shifts caused by upstream compression. This design yields compressed layers that more faithfully
 097 preserve the functional behavior of the uncompressed model, enabling effective post-training com-
 098 pression of billion-parameter networks without retraining. Our contributions can be summarized as
 099 follows:

- 100 • **A fast compression method** that improves upon prior SVD-based approaches, with neg-
 101 ligible overhead compared to optimization-heavy baselines such as DobiSVD Wang et al.
 102 (2025a).
- 103 • **A novel objective formulation** that anchors compressed layers to the original outputs
 104 while explicitly modeling input distribution shifts, thereby better preserving functional
 105 equivalence to the uncompressed model.
- 106 • **Comprehensive evaluation** across large-scale language models, demonstrating favorable
 107 trade-offs between compression ratio and accuracy, and outperforming existing SVD-based
 108 baselines.

108

2 RELATED WORK

110 Low-rank factorization, e.g., via singular value decomposition (SVD), has emerged as a promising
 111 direction for compressing large pretrained models. Compared to pruning or quantization, SVD-
 112 based methods offer several practical advantages. First, factorizing a weight matrix into low-rank
 113 components yields a *structured* representation that reduces both parameters and compute. The fac-
 114 torized form enables commuting multiplications— $(UV^\top)X = U(V^\top X)$ —which reduces memory
 115 requirement and can be implemented efficiently on existing accelerators. Second, unlike pruning,
 116 which often introduces irregular sparsity, or quantization, which requires specialized kernels for
 117 speedup, SVD-based methods produce dense but smaller matrices that integrate seamlessly with
 118 standard linear algebra libraries. Finally, they can be applied post-training with only small calibra-
 119 tion samples (often a few hundred), making them particularly attractive for compressing billion-
 120 parameter models where retraining is infeasible. Recent methods such as ASVD (Yuan et al., 2023),
 121 SVD-LLM (Wang et al., 2025d), AdaSVD (Li et al., 2025), SVD-LLM V2 (Wang et al., 2025b) and
 122 Dobi-SVD (Wang et al., 2025a) have demonstrated the viability of this approach at scale in large
 123 language models.

124 Based on the optimization objective, SVD-based compression methods can be grouped into the
 125 following categories :

126 **Input-agnostic (direct) SVD.** The simplest approach applies a truncated singular value decom-
 127 position to the weight matrix W , replacing it by a rank- r approximation W' constructed from its
 128 top singular components (Halko et al., 2011; Sainath et al., 2013). This method is appealing for its
 129 simplicity and minimal data dependence. However, direct SVD treats all input directions uniformly,
 130 ignoring the fact that in deep networks, the actual input activations X lie in a highly anisotropic
 131 subspace. In such settings, the singular vectors preserved by SVD may not align with the task-
 132 relevant activation patterns or the dominant subspace of X , leading to suboptimal approximations.
 133 Indeed, empirical studies in neural network compression consistently find that direct SVD often un-
 134 derperforms data-aware variants tuned to activation statistics (e.g. Chen et al. (2021); Idelbayev &
 135 Carreira-Perpiñán (2020)). More broadly, analyses of neural anisotropy directions suggest that deep
 136 models naturally concentrate representation into narrow subspaces, reinforcing why input-agnostic
 137 approximations are misaligned with the true geometry of activations Ortiz-Jiménez et al. (2020).

138 **Activation-aware factorization.** To incorporate the geometry of the inputs actually seen by the
 139 network, activation-aware methods optimize the reconstruction
 140

$$\min_{W':\text{rank}(W')=r} \|WX - W'X\|_F^2,$$

141 where X are activations collected from the original, uncompressed model. Examples include
 142 Drone (Chen et al., 2021), ASVD (Yuan et al., 2023), SVD-LLM (Wang et al., 2025d), AdaSVD (Li
 143 et al., 2025), and SVD-LLM V2 (Wang et al., 2025b). By preserving the action of W on its occupied
 144 input subspace, these approaches are often more faithful than direct SVD. However, their perfor-
 145 mance hinges on the representativeness of the calibration set used to obtain X . If calibration data
 146 are narrow or unaligned with downstream usage, compressed models may overfit to the sampled
 147 geometry and fail to generalize. Related activation-matching objectives also appear in structured
 148 pruning frameworks, such as FLAP (An et al., 2024), which similarly leverage activation statistics
 149 to guide parameter removal.

150 **Shift-aware factorization.** A key limitation of activation-aware approaches is that they optimize
 151 with respect to the original activations X , even though, in a sequentially compressed model, later
 152 layers actually receive shifted inputs X' . To account for this, shift-aware methods, e.g. Dobi-
 153 SVD (Wang et al., 2025a), optimize

$$\min_{W':\text{rank}(W')=r} \|WX' - W'X'\|_F^2,$$

154 using activations from the partially compressed network. By aligning the approximation to the dis-
 155 tribution the layer truly encounters, these methods can mitigate error propagation through the stack.
 156 Their drawback, however, is that when upstream compression has already degraded representations,
 157 anchoring solely to X' risks amplifying divergence from the original mapping. In addition, batch-
 158 based surrogates for X' are often noisy or unrepresentative, which can introduce instability into the

approximation. As a result, shift-aware objectives alone provide only a partial solution. Related ideas also appear implicitly in earlier CNN low-rank factorization (Denton et al., 2014; Jaderberg et al., 2014), where activations were collected after partial compression, and in layer-wise distillation methods (e.g., TinyBERT (Jiao et al., 2020)), where the compressed model is aligned to the teacher using its own inputs.

Beyond the choice of approximation objective, the effectiveness of low-rank factorization depends critically on how ranks are distributed across layers. Uniform allocation ignores heterogeneity in both compressibility and functional importance. Adaptive strategies such as AdaSVD (Li et al., 2025) leverage layer-importance signals to allocate more rank where needed, in line with importance-based pruning approaches such as ShortGPT (Men et al., 2024). SVD-LLM V2 (Wang et al., 2025b) instead proposed a heuristic that reallocates rank based on the truncation loss $\|WX - W'X\|_F^2$ observed after uniform compression. Earlier work on CNNs has also explored learning per-layer ranks directly via group sparsity regularization over singular values (Idelbayev & Carreira-Perpinán, 2020), showing clear gains over uniform allocation. Differentiable allocation schemes have also been explored (e.g., in Dobi-SVD (Wang et al., 2025a)), but these typically require costly optimization and rely on unstable batch-level statistics. Collectively, these advances highlight that compression quality depends not only on the local objective but also on *where* and *how* rank is assigned.

3 AA-SVD

In this section we present our compression framework, **AA-SVD** (Anchored and Adaptive SVD). The central idea is to construct low-rank approximations of each linear transformation in a pretrained network such that the compressed model remains *locally faithful* to the original network, while simultaneously adapting to the distributional shifts induced by upstream compression.

Formally, we denote a weight matrix at layer ℓ by $W \in \mathbb{R}^{m \times n}$, with input activations $X \in \mathbb{R}^{n \times k}$ and outputs $WX \in \mathbb{R}^{m \times k}$, where k is the number of calibration samples. After compressing earlier layers, the same layer instead receives shifted activations $X' \in \mathbb{R}^{n \times k}$, producing outputs $W'X'$. Our objective is to replace W with a rank-constrained approximation $W' \in \mathbb{R}^{m \times n}$, where $\text{rank}(W') = r \ll \min(m, n)$, such that $W'X'$ remains close to WX . In this way, **AA-SVD** enforces that the compressed layer continues to behave like the original one *in the local neighborhood defined by its actual inputs*, while still anchored to the outputs of the uncompressed model.

3.1 OBJECTIVE

Our goal is to compress each linear transformation while ensuring that the resulting network remains *locally faithful* to the original model under the inputs it will actually encounter. Concretely, for a weight matrix $W \in \mathbb{R}^{m \times n}$ with original inputs $X \in \mathbb{R}^{n \times k}$ and shifted inputs $X' \in \mathbb{R}^{n \times k}$ (after upstream compression), we seek a low-rank approximation $W' \in \mathbb{R}^{m \times n}$ that solves

$$\min_{W': \text{rank}(W')=r} \|WX - W'X'\|_F^2.$$

This objective enforces that the compressed outputs $W'X'$ stay close to the original outputs WX , anchoring the compressed network to the behavior of the uncompressed one while simultaneously adapting to the shifted input distribution. By explicitly constraining $\text{rank}(W') = r$, the problem is well-posed as a low-rank regression: we seek the best rank- r approximation of the mapping from X' to WX .

Theorem 3.1 (Low-rank approximation with upstream-modified inputs). *Let $W \in \mathbb{R}^{m \times d}$ be a fixed weight matrix and $X, X' \in \mathbb{R}^{d \times N}$ be two sets of input activations (columns are samples). Define*

$$A := XX'^\top \in \mathbb{R}^{d \times d}, \quad B := X'X'^\top \in \mathbb{R}^{d \times d}.$$

Fix a target rank $k \in \mathbb{N}$. Consider the optimization problem

$$\min_{\text{rank}(W') \leq k} \|WX - W'X'\|_F^2. \quad (1)$$

Let $B = R^\top R$ be a Cholesky factorization with R upper triangular, and define $M := WAR^{-1}$. If $M = U\Sigma V^\top$ is a thin singular value decomposition, then an optimal solution to equation 1 is

$$W'^* = (U_k \Sigma_k V_k^\top) R^{-1},$$

216 **Algorithm 1 AA-SVD** Low-rank compression

217 **Require:** Weight matrix $W \in \mathbb{R}^{m \times d}$, original inputs $X \in \mathbb{R}^{d \times N}$, current inputs $X' \in \mathbb{R}^{d \times N}$,
 218 target rank k
 219 1: Compute covariances $A = XX'^\top$ and $B = X'X'^\top$
 220 2: Cholesky factorization: $B = R^\top R$
 221 3: Compute $M = WAR^{-1}$
 222 4: Truncated SVD: $M \approx U_k \Sigma_k V_k^\top$
 223 5: Return $W' = (U_k \Sigma_k V_k^\top) R^{-1}$ or factorized matrices $U = U_k \Sigma_k$ and $V = V_k^\top R^{-1}$

225
 226 where U_k, Σ_k, V_k are the top- k blocks of the SVD. The minimum objective value is
 227

$$228 \quad \|WX\|_F^2 - \|M\|_F^2 + \sum_{i>k} \sigma_i(M)^2,$$

230 where $\sigma_i(M)$ are the singular values of M .
 231

232 *Proof.* Expanding the squared Frobenius norm gives
 233

$$234 \quad \|WX - W'X'\|_F^2 = \text{tr}(W'BW'^\top) - 2 \text{tr}(WAW'^\top) + \|WX\|_F^2.$$

235 Since $B = R^\top R$, the first term is $\|W'R\|_F^2$. Completing the square yields
 236

$$237 \quad \|W'R - WAR^{-1}\|_F^2 - \|WAR^{-1}\|_F^2 + \|WX\|_F^2.$$

238 Thus minimizing equation 1 is equivalent to minimizing $\|W'R - M\|_F^2$ subject to $\text{rank}(W'R) \leq k$,
 239 where $M = WAR^{-1}$. Because R is invertible, $\text{rank}(W'R) = \text{rank}(W')$. By the Eckart–Young–
 240 Mirsky theorem, the optimal approximation is $U_k \Sigma_k V_k^\top$, yielding
 241

$$242 \quad W'^* = (U_k \Sigma_k V_k^\top) R^{-1},$$

243 and the minimal value as claimed. \square
 244

245 **Corollary 3.2** (Classical whitening as a special case). *If $X' = X$, then $A = B$ and $M = WB^{1/2} =$
 246 WR^\top . The solution reduces to*

$$247 \quad W'^* = (WB^{1/2})_k B^{-1/2},$$

248 the standard whitening-based low-rank regression solution.
 249

250 *Remark 3.3* (Rank-deficient X'). If $B \succeq 0$ is singular, the Cholesky factorization does not exist.
 251 In this case replace R^{-1} by the Moore–Penrose factor $B^{+1/2}$, or equivalently use a Tikhonov–
 252 regularized factorization $B + \varepsilon I = R_\varepsilon^\top R_\varepsilon$ and let $\varepsilon \rightarrow 0^+$. The same argument then shows that
 253

$$254 \quad W'^* = (U_k \Sigma_k V_k^\top) B^{+1/2}, \quad M := WAB^{+1/2},$$

255 is a minimum-norm optimizer, with minimal value given by the same formula.
 256

257 Theorem 3.1 establishes that the optimal rank- k compressed operator is obtained by whitening the
 258 modified inputs X' via their covariance, projecting the cross-term WA into this whitened space,
 259 applying truncated SVD, and mapping back. This closed-form solution generalizes the classical
 260 whitening construction ($X' = X$) and can be implemented efficiently with a Cholesky factorization.
 261 Importantly, our formulation operates only on the covariance matrices XX'^\top and $X'X'^\top$ rather than
 262 the raw activations themselves. This is especially advantageous when the number of samples is large
 263 (e.g. in our setting with 256 samples of length 2048, corresponding to over half a million effective
 264 columns), since the covariance matrices are fixed-size $d \times d$ regardless of the batch length. For
 265 clarity, Algorithm 1 summarizes the procedure.

266 **4 EXPERIMENTS**
 267

268 We empirically evaluate our method on large-scale language models from the LLaMA family,
 269 focusing primarily on LLaMA-7B and extending to larger variants to assess scalability. Our goals are
 threefold: (i) to compare against existing SVD-based and low-rank baselines in terms of perplexity

270
 271 Table 1: Comparison of **AA-SVD** with SOTA methods for SVD-based compression of Llama-7B
 272 on two language modeling tasks and six common sense reasoning datasets (zero-shot evaluation).
 273 Best performance is marked in bold. \dagger uses LoRA fine-tuning, while \ddagger uses dynamic or non-uniform
 274 ratio allocation.

276 Ratio	277 Method	278 PPL (\downarrow)		279 Accuracy (\uparrow)					
		280 Wiki2	281 PTB	282 Openb.	283 ARC.e	284 ARC.c	285 WinoG.	286 PIQA	287 MathQA
288 1.0	289 Baseline	290 5.68	291 8.79	292 0.34	293 0.75	294 0.42	295 0.69	296 0.79	297 0.27
298 0.8	299 ASVD	300 11.14	301 16.55	302 0.25	303 0.53	304 0.27	305 0.64	306 0.68	307 0.24
	308 SVD-LLM \dagger	309 7.94	310 16.22	311 0.22	312 0.58	313 0.29	314 0.63	315 0.69	316 0.24
	317 Dobi-SVD \ddagger	318 8.54	319 14.83	320 0.26	321 0.59	322 0.31	323 0.66	324 0.70	325 0.23
	326 AA-SVD	327 7.67	328 16.11	329 0.29	330 0.64	331 0.33	332 0.65	333 0.69	334 0.24
335 0.6	336 ASVD	337 1407	338 3292	339 0.13	340 0.28	341 0.22	342 0.48	343 0.55	344 0.19
	345 SVD-LLM \dagger	346 13.11	347 63.75	348 0.19	349 0.42	350 0.25	351 0.58	352 0.60	353 0.21
	354 Dobi-SVD \ddagger	355 13.54	356 46.38	357 0.22	358 0.41	359 0.27	360 0.58	361 0.61	362 0.23
	363 AA-SVD	364 12.19	365 35.32	366 0.19	367 0.46	368 0.23	369 0.59	370 0.60	371 0.23
372 0.4	373 ASVD	374 57057	375 45218	376 0.12	377 0.26	378 0.21	379 0.49	380 0.53	381 0.18
	382 SVD-LLM \dagger	383 53.74	384 438.58	385 0.14	386 0.28	387 0.22	388 0.50	389 0.55	390 0.21
	391 Dobi-SVD \ddagger	392 46.18	393 238.91	394 0.15	395 0.31	396 0.20	397 0.52	398 0.54	399 0.22
	400 AA-SVD	401 29.54	402 214.84	403 0.15	404 0.32	405 0.20	406 0.50	407 0.54	408 0.22
409 0.2	410 SVD-LLM \dagger	411 1349	412 --	413 0.07	414 0.03	415 --	416 0.04	417 0.07	418 0.01
	419 AA-SVD	420 144.03	421 394.52	422 0.14	423 0.28	424 0.22	425 0.51	426 0.52	427 0.22

295 and downstream reasoning accuracy, (ii) to quantify efficiency improvements in memory footprint
 296 and inference cost, and (iii) to analyze the contribution of different design choices, including calibra-
 297 tion set size, dynamic rank allocation, and post-compression refinements. Unless noted otherwise,
 298 all compression methods use a calibration set of 256 samples drawn from the WikiText2 dataset,
 299 following prior work. Performance is evaluated using two complementary metrics: (i) *language*
 300 *modeling perplexity*, measured on standard corpora including WikiText2 (Merity et al., 2016), and
 301 PTB (Marcinkiewicz, 1994); and (ii) *accuracy on commonsense reasoning*, measured on bench-
 302 marks such as Winogrande (Sakaguchi et al., 2020), PIQA (Bisk et al., 2020), MathQA (Amini
 303 et al., 2019), ARC-Easy and ARC-Challenge (Clark et al., 2018), and OpenBookQA (Mihaylov
 304 et al., 2018).

305 306 4.1 MAIN RESULTS

308 We evaluate the performance of **AA-SVD** with compression ratios ranging from 20% to 80%. Ta-
 309 ble 1 reports perplexity on two language modeling corpora (WikiText2 and PTB) and accuracy
 310 across six common sense reasoning benchmarks, under varying compression ratios. We compare
 311 against other SVD-based compression methods - ASVD, SVD-LLM, and DoBi-SVD.

312 At a high compression ratio of 0.8, AA-SVD already improves over all baselines in terms of average
 313 accuracy while maintaining perplexity close to the best-performing methods. For instance, AA-SVD
 314 yields the lowest perplexity of 7.67 and higher reasoning accuracy than DoBi-SVD on four out of
 315 six tasks, demonstrating robustness across both metrics.

317 As compression becomes more aggressive, the gap between AA-SVD and competing methods
 318 widens. At ratio 0.6, AA-SVD reduces perplexity substantially (WikiText2: 12.19 vs. 13.54 for
 319 DoBi-SVD, while PTB: 35.32 vs. 46.38), while either matching or outperforming in reasoning
 320 accuracy. At ratio 0.4, AA-SVD achieves a perplexity reduction of nearly 20% over DoBi-SVD and
 321 consistently ranks among the top two methods on all reasoning tasks.

322 The advantage is most pronounced at the extreme ratio of 0.2. Here, competing approaches collapse,
 323 with SVD-LLM reporting almost degenerate results. In contrast, AA-SVD remains functional, pre-
 324 serving non-trivial accuracy (e.g., PIQA: 0.51, ARC.c: 0.22) and maintaining perplexities below

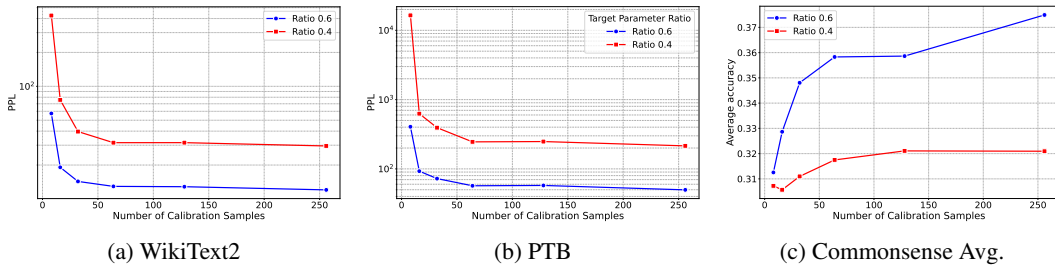


Figure 1: Impact of calibration set size on compression performance. Performance is measured by perplexity on WikiText2 and PTB, and average accuracy across six commonsense reasoning tasks.

400. This indicates that the combination of shift anchoring and dynamic rank allocation stabilizes compression even in highly resource-constrained regimes.

Overall, these results highlight that AA-SVD offers the best trade-off between language modeling fidelity and downstream reasoning ability, especially when compression is aggressive. Notably, our method avoids the collapse observed in prior SVD-based approaches at low ranks, underscoring the importance of accounting for both original outputs and shifted inputs.

4.2 MEMORY AND SPEEDUP

Low-rank factorization reduces both parameter count and compute cost by replacing a dense matrix with the product of two thin factors. Consider a linear layer $W \in \mathbb{R}^{m \times n}$. The original layer requires mn parameters and $O(mn)$ FLOPs per forward pass. A rank- r factorization stores $mr + nr$ parameters and incurs $O(mr + nr)$ FLOPs, which is cheaper whenever $r \ll \min(m, n)$. The effective compression ratio is

$$\rho = \frac{mr + nr}{mn}.$$

For example, with $m = n = 4096$ and $r = 512$ ($\rho = 0.125$), the parameter count drops from 16.8M to 4.2M (a $4\times$ reduction), and FLOPs per forward pass reduce by the same factor.

Beyond weights and FLOPs, low-rank factorization can also reduce the memory footprint of the key-value (KV) cache during autoregressive inference. Since attention projections are compressed, the activations stored in the cache scale with r rather than n , yielding proportional savings in both memory and bandwidth. As highlighted in SVD-LLM (Wang et al., 2025d) and follow-up works, this reduction is crucial for long-context inference where KV-cache dominates memory usage.

Our method (AA-SVD) preserves this structural efficiency: the cost of computing compressed weights is incurred once during compression, while inference cost and KV-cache size match those of standard low-rank layers. Thus, AA-SVD offers the same runtime and memory benefits as prior SVD-based methods, with its main advantage lying in improved approximation quality under aggressive compression.

4.3 ABLATIONS AND ANALYSIS

Impact of Number of Calibration Samples. Figure 1 illustrates the impact of calibration set size on compression performance. We report perplexity on WikiText2 (Fig. 1a) and PTB (Fig. 1b), as well as the average accuracy across six reasoning tasks (Fig. 1c), for compression ratios 0.6 and 0.4. Performance improves steadily with additional samples, but perplexity quickly saturates beyond ~ 64 examples. Notably, even with as few as 64 samples, AA-SVD remains stable and delivers competitive results, indicating that only a modest calibration set is required. For commonsense reasoning, particularly at the higher compression ratio, larger calibration sets provide incremental gains, suggesting room for further improvement in more data-rich settings.

Error Evolution Across Layers. To better understand how compression affects the internal representations, we track the discrepancy between the original and compressed models across depth. Figure 2 plots layerwise *cosine distance* between original and compressed features (WX vs. $W'X'$);

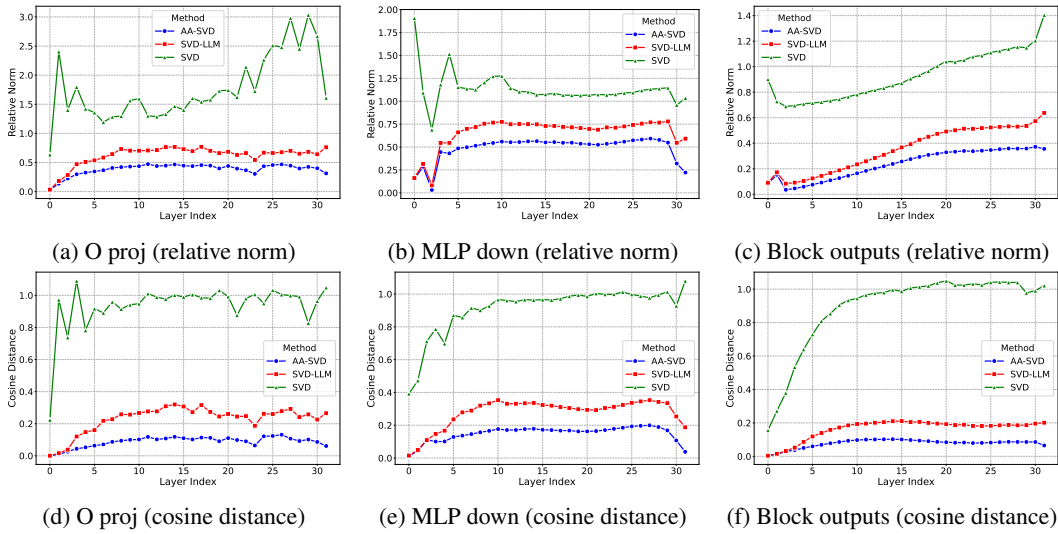


Figure 2: Layerwise error evolution. Top row: relative norm difference $\|WX - W'X'\|_F / \|WX\|_F$. Bottom row: cosine distance between WX and $W'X'$. Results are shown separately for query (Q) projections, MLP down-projections, and block outputs.

lower is better) alongside the *relative norm* error $\|WX - W'X'\|_F / \|WX\|_F$. We compress Llama-7B model at 60% compression ratio with **AA-SVD** and compare it with naive SVD as well as SVD-LLM. We use only 64 calibration samples from WikiText2 for each method. We show results for output projections, MLP down-projections, and transformer layer/block outputs. Across all methods, AA-SVD consistently achieves the **lowest cosine distance** and **lowest relative norm** error, while direct SVD exhibits the largest divergences, especially in deeper layers where error accumulates. SVD-LLM lies in between but still shows increasing gap with depth. This reduction in layerwise error directly translates into stronger end-task performance. For example, AA-SVD achieves a perplexity of 12.92 on WikiText2 and 57.02 on PTB, compared to (14.38 / 77.71) for SVD-LLM and (50714 / 60103) with naive SVD (indicating catastrophic degradation). These results confirm that stabilizing error growth across depth is critical for preserving downstream accuracy. Anchoring to both original outputs and shifted inputs curbs error growth and preserves feature geometry throughout the network.

5 CONCLUSION

We introduced a fast, post-training framework for compressing large language and vision-language models using rank-constrained SVD. Unlike prior approaches that rely exclusively on original inputs or shifted activations, our method unifies both perspectives: it anchors each compressed layer to the outputs of the uncompressed network while adapting to the inputs that arise after upstream compression. This leads to closed-form solutions with a rank constraint, efficient to compute from a small calibration set. Extensive experiments on the LLaMA family and commonsense reasoning benchmarks show that our approach consistently outperforms direct and activation-aware SVD methods, as well as shift-only approaches such as DobiSVD. At low compression ratios, our method preserves accuracy with negligible loss, while under aggressive compression it widens the gap to baselines. Overall, our study demonstrates that careful design of the compression objective and rank allocation strategy enables billion-parameter models to be compressed quickly and effectively without retraining. We hope this work contributes toward practical, accessible deployment of large-scale pretrained models, and inspires further exploration of hybrid objectives and allocation schemes for efficient model compression.

432 REFERENCES
433

434 Josh Achiam, Steven Adler, Sandhini Agarwal, Lama Ahmad, Ilge Akkaya, Florencia Leoni Ale-
435 man, Diogo Almeida, Janko Altenschmidt, Sam Altman, Shyamal Anadkat, et al. Gpt-4 technical
436 report. *arXiv preprint arXiv:2303.08774*, 2023.

437 Aida Amini, Saadia Gabriel, Peter Lin, Rik Koncel-Kedziorski, Yejin Choi, and Hannaneh Ha-
438 jishirzi. Mathqa: Towards interpretable math word problem solving with operation-based for-
439 malisms. *arXiv preprint arXiv:1905.13319*, 2019.

440 Yongqi An, Xu Zhao, Tao Yu, Ming Tang, and Jinqiao Wang. Fluctuation-based adaptive struc-
441 tured pruning for large language models. In *Proceedings of the AAAI Conference on Artificial*
442 *Intelligence*, volume 38, pp. 10865–10873, 2024.

443 Saleh Ashkboos, Maximilian L Croci, Marcelo Gennari do Nascimento, Torsten Hoefer, and James
444 Hensman. SliceGPT: Compress large language models by deleting rows and columns. *arXiv*
445 *preprint arXiv:2401.15024*, 2024.

446 Yonatan Bisk, Rowan Zellers, Jianfeng Gao, and Yejin Choi. Piqa: Reasoning about physical com-
447 monsense in natural language. In *Proceedings of the AAAI Conference on Artificial Intelligence*,
448 volume 34, pp. 7432–7439, 2020.

449 Patrick Chen, Hsiang-Fu Yu, Inderjit Dhillon, and Cho-Jui Hsieh. Drone: Data-aware low-rank
450 compression for large nlp models. *Advances in neural information processing systems*, 34:29321–
451 29334, 2021.

452 Yu Cheng, Duo Wang, Pan Zhou, and Tao Zhang. A survey of model compression and acceleration
453 for deep neural networks. *arXiv preprint arXiv:1710.09282*, 2017.

454 Yu Cheng, Duo Wang, Pan Zhou, and Tao Zhang. Model compression and acceleration for deep
455 neural networks: The principles, progress, and challenges. *IEEE Signal Processing Magazine*, 35
456 (1):126–136, 2018.

457 Peter Clark, Isaac Cowhey, Oren Etzioni, Tushar Khot, Ashish Sabharwal, Carissa Schoenick, and
458 Oyvind Tafjord. Think you have solved question answering? try arc, the ai2 reasoning challenge.
459 In *Proceedings of EMNLP*, pp. 279–290, 2018.

460 Misha Denil, Babak Shakibi, Laurent Dinh, and Nando de Freitas. Predicting parameters in deep
461 learning. In *Advances in neural information processing systems*, volume 26, 2013.

462 Emily L Denton, Wojciech Zaremba, Joan Bruna, Yann LeCun, and Rob Fergus. Exploiting linear
463 structure within convolutional networks for efficient evaluation. In *Advances in neural informa-
464 tion processing systems*, volume 27, 2014.

465 Tim Dettmers, Mike Lewis, Sam Shleifer, and Luke Zettlemoyer. Llm.int8(): 8-bit matrix multipli-
466 cation for transformers at scale. In *Advances in Neural Information Processing Systems*, 2022.

467 Tim Dettmers, Artidoro Pagnoni, Ari Holtzman, and Luke Zettlemoyer. Qlora: Efficient finetuning
468 of quantized llms. *Advances in neural information processing systems*, 36:10088–10115, 2023.

469 Alexey Dosovitskiy, Lucas Beyer, Alexander Kolesnikov, Dirk Weissenborn, Xiaohua Zhai, Thomas
470 Unterthiner, Mostafa Dehghani, Matthias Minderer, Georg Heigold, Sylvain Gelly, Jakob Uszko-
471 reit, and Neil Houlsby. An image is worth 16x16 words: Transformers for image recognition at
472 scale. In *International Conference on Learning Representations*, 2021.

473 Jonathan Frankle and Michael Carbin. The lottery ticket hypothesis: Finding sparse, trainable neural
474 networks. In *International Conference on Learning Representations*, 2019.

475 Elias Frantar and Dan Alistarh. SparseGPT: Massive language models can be accurately pruned in
476 one-shot. *arXiv preprint arXiv:2301.00774*, 2023.

477 Elias Frantar, Saleh Ashkboos, Pierre Stock, and Dan Alistarh. Gptq: Accurate post-training quan-
478 tization for generative pretrained transformers. *arXiv preprint arXiv:2210.17323*, 2022.

486 Nathan Halko, Per-Gunnar Martinsson, and Joel A. Tropp. *Finding Structure with Randomness:*
 487 *Probabilistic Algorithms for Constructing Approximate Matrix Decompositions*. 2011.

488

489 Song Han, Jeff Pool, John Tran, and William J Dally. Learning both weights and connections for
 490 efficient neural networks. In *Advances in neural information processing systems*, volume 28,
 491 2015.

492 Geoffrey Hinton, Oriol Vinyals, and Jeff Dean. Distilling the knowledge in a neural network. In
 493 *NeurIPS Deep Learning Workshop*, 2015.

494

495 Itay Hubara, Matthieu Courbariaux, Daniel Soudry, Ran El-Yaniv, and Yoshua Bengio. Quantized
 496 neural networks: Training neural networks with low precision weights and activations. *Journal*
 497 *of Machine Learning Research*, 18(1):6869–6898, 2017.

498

499 Yerlan Idelbayev and Miguel A Carreira-Perpiñán. Low-rank compression of neural nets: Learning
 500 the rank of each layer. In *Proceedings of the IEEE/CVF conference on computer vision and*
 501 *pattern recognition*, pp. 8049–8059, 2020.

502

503 Max Jaderberg, Andrea Vedaldi, and Andrew Zisserman. Speeding up convolutional neural networks
 504 with low rank expansions. In *Proceedings of the British Machine Vision Conference*, 2014.

505

506 Xiaoqi Jiao, Yichun Yin, Lifeng Shang, Xin Jiang, Xiao Chen, Linlin Li, Fang Wang, and Qun Liu.
 507 Tinybert: Distilling bert for natural language understanding. In *Findings of the Association for*
 508 *Computational Linguistics: EMNLP 2020*, pp. 4163–4174, 2020.

509

510 Jared Kaplan, Sam McCandlish, Tom Henighan, Tom B Brown, Benjamin Chess, Rewon Child,
 511 Scott Gray, Alec Radford, Jeffrey Wu, and Dario Amodei. Scaling laws for neural language
 512 models. *arXiv preprint arXiv:2001.08361*, 2020.

513

514 Zhiteng Li, Mingyuan Xia, Jingyuan Zhang, Zheng Hui, Linghe Kong, Yulun Zhang, and Xiaokang
 515 Yang. Adasvd: Adaptive singular value decomposition for large language models. 2025.

516

517 Ji Lin, Jiaming Tang, Haotian Tang, Shang Yang, Wei-Ming Chen, Wei-Chen Wang, Guangxuan
 518 Xiao, Xingyu Dang, Chuang Gan, and Song Han. Awq: Activation-aware weight quantization
 519 for on-device llm compression and acceleration. *Proceedings of machine learning and systems*,
 520 6:87–100, 2024.

521

522 Haotian Liu, Chunyuan Li, Qingyang Wu, and Yong Jae Lee. Visual instruction tuning. *Advances*
 523 *in Neural Information Processing Systems*, 36, 2023.

524

525 Xinyin Ma, Gongfan Fang, and Xinchao Wang. Llm-pruner: On the structural pruning of large
 526 language models. *Advances in neural information processing systems*, 36:21702–21720, 2023.

527

528 Mary Ann Marcinkiewicz. Building a large annotated corpus of english: The penn treebank. *Using*
 529 *Large Corpora*, 273:31, 1994.

530

531 Xin Men, Mingyu Xu, Qingyu Zhang, Bingning Wang, Hongyu Lin, Yaojie Lu, Xianpei Han, and
 532 Weipeng Chen. Shortgpt: Layers in large language models are more redundant than you expect.
 533 *arXiv preprint arXiv:2403.03853*, 2024.

534

535 Stephen Merity, Caiming Xiong, James Bradbury, and Richard Socher. Pointer sentinel mixture
 536 models. *arXiv preprint arXiv:1609.07843*, 2016.

537

538 Todor Mihaylov, Peter Clark, Tushar Khot, and Ashish Sabharwal. Can a suit of armor conduct
 539 electricity? a new dataset for open book question answering. In *Proceedings of EMNLP*, pp.
 2381–2391, 2018.

540

541 Guillermo Ortiz-Jiménez, Apostolos Modas, Seyed-Mohsen Moosavi, and Pascal Frossard. Neural
 542 anisotropy directions. *Advances in Neural Information Processing Systems*, 33:17896–17906,
 543 2020.

544

545 David Patterson, Joseph Gonzalez, Quoc Le, Chen Liang, Lluís Munguia, Daniel Rothchild, David R
 546 So, Maud Texier, and Jeffrey Dean. Carbon emissions and large neural network training. *arXiv*
 547 *preprint arXiv:2104.10350*, 2021.

540 Alec Radford, Jong Wook Kim, Chris Hallacy, Aditya Ramesh, Gabriel Goh, Sandhini Agar-
 541 wal, Girish Sastry, Amanda Askell, Pamela Mishkin, Jack Clark, Gretchen Krueger, and Ilya
 542 Sutskever. Learning transferable visual models from natural language supervision. In *Inter-
 543 national Conference on Machine Learning*, pp. 8748–8763. PMLR, 2021.

544

545 Tara N Sainath, Brian Kingsbury, Vikas Sindhwani, Ebru Arisoy, and Bhuvana Ramabhadran. Low-
 546 rank matrix factorization for deep neural network training with high-dimensional output targets.
 547 In *2013 IEEE international conference on acoustics, speech and signal processing*, pp. 6655–
 548 6659. IEEE, 2013.

549

550 Keisuke Sakaguchi, Ronan Le Bras, Chandra Bhagavatula, and Yejin Choi. Winogrande: An adver-
 551 sarial winograd schema challenge at scale. In *Proceedings of the AAAI Conference on Artificial
 552 Intelligence*, volume 34, pp. 8732–8740, 2020.

553

554 Chengxi Ye Tai, Tong Xiao, Yi Zhang, and Xiaogang Wang. Convolutional neural networks with
 555 low-rank regularization. In *International Conference on Learning Representations*, 2015.

556

557 Hugo Touvron, Matthieu Cord, Matthijs Douze, Francisco Massa, Alexandre Sablayrolles, and
 558 Hervé Jégou. Training data-efficient image transformers & distillation through attention. In
 559 *International Conference on Machine Learning*, pp. 10347–10357. PMLR, 2021.

560

561 Hugo Touvron, Louis Martin, Kevin Stone, et al. Llama: Open and efficient foundation language
 562 models. *arXiv preprint arXiv:2302.13971*, 2023.

563

564 Qinsi Wang, Jinghan Ke, Masayoshi Tomizuka, Yiran Chen, Kurt Keutzer, and Chenfeng Xu. Dobi-
 565 svd: Differentiable svd for llm compression and some new perspectives. In *ICLR*, 2025a.

566

567 X. Wang et al. Svd-llm v2: Optimizing singular value truncation for llm compression. In *NAACL
 568 Long*, 2025b.

569

570 Xin Wang, Samiul Alam, Zhongwei Wan, Hui Shen, and Mi Zhang. Svd-llm v2: Optimizing singu-
 571 lar value truncation for large language model compression. In *Proceedings of the 2025 Conference
 572 of the Nations of the Americas Chapter of the Association for Computational Linguistics: Human
 573 Language Technologies (Volume 1: Long Papers)*, pp. 4287–4296, 2025c.

574

575 Xin Wang, Yu Zheng, Zhongwei Wan, and Mi Zhang. SVD-LLM: Truncation-aware singular
 576 value decomposition for large language model compression. In *International Conference on
 577 Learning Representations (ICLR)*, 2025d. URL <https://openreview.net/forum?id=LYI1Uouhdt>.

578

579 Xiaohan Xu, Ming Li, Chongyang Tao, Tao Shen, Reynold Cheng, Jinyang Li, Can Xu, Dacheng
 580 Tao, and Tianyi Zhou. A survey on knowledge distillation of large language models. *arXiv
 581 preprint arXiv:2402.13116*, 2024.

582

583 Zhihang Yuan, Yuzhang Shang, Yue Song, Qiang Wu, Yan Yan, and Guangyu Sun. Asvd:
 584 Activation-aware singular value decomposition for compressing large language models. *arXiv
 585 preprint arXiv:2312.05821*, 2023.

586

587 Susan Zhang, Stephen Roller, Naman Goyal, Mikel Artetxe, Moya Chen, Shuohui Chen, Christo-
 588 pher Dewan, Mona Diab, Xian Li, Xi Victoria Lin, et al. Opt: Open pre-trained transformer
 589 language models. *arXiv preprint arXiv:2205.01068*, 2022.

590

591 Xunyu Zhu, Jian Li, Yong Liu, Can Ma, and Weiping Wang. A survey on model compression
 592 for large language models. *Transactions of the Association for Computational Linguistics*, 12:
 593 1556–1577, 2024.

594

595

596

597

598

599

600

601

602

603

604

605

606

607

608

609

610

611

612

613

614

615

616

617

618

619

620

621

622

623

624

625

626

627

628

629

630

631

632

633

634

635

636

637

638

639

640

641

642

643

644

645

646

647

648

649

650

651

652

653

654

655

656

657

658

659

660

661

662

663

664

665

666

667

668

669

670

671

672

673

674

675

676

677

678

679

680

681

682

683

684

685

686

687

688

689

690

691

692

693

694

695

696

697

698

699

700

701

702

703

704

705

706

707

708

709

710

711

712

713

714

715

716

717

718

719

720

721

722

723

724

725

726

727

728

729

730

731

732

733

734

735

736

737

738

739

740

741

742

743

744

745

746

747

748

749

750

751

752

753

754

755

756

757

758

759

760

761

762

763

764

765

766

767

768

769

770

771

772

773

774

775

776

777

778

779

780

781

782

783

784

785

786

787

788

789

790

791

792

793

794

795

796

797

798

799

800

801

802

803

804

805

806

807

808

809

810

811

812

813

814

815

816

817

818

819

820

821

822

823

824

825

826

827

828

829

830

831

832

833

834

835

836

837

838

839

840

841

842

843

844

845

846

847

848

849

850

851

852

853

854

855

856

857

858

859

860

861

862

863

864

865

866

867

868

869

870

871

872

873

874

875

876

877

878

879

880

881

882

883

884

885

886

887

888

889

890

891

892

893

894

895

896

897

898

899

900

901

902

903

904

905

906

907

908

909

910

911

912

913

914

915

916

917

918

919

920

921

922

923

924

925

926

927

928

929

930

931

932

933

934

935

936

937

938

939

940

941

942

943

944

945

946

947

948

949

950

951

952

953

954

955

956

957

958

959

960

961

962

963

964

965

966

967

968

969

970

971

972

973

974

975

976

977

978

979

980

981

982

983

984

985

986

987

988

989

990

991

992

993

994

995

996

997

998

999

1000